Universidade de São Paulo
Instituto de Física

Vínculos Cosmológicos com o Auxílio do Efeito Sachs-Wolfe Integrado

Arthur Diniz Meirelles

Orientador: Prof. Dr. Edivaldo Moura Santos
Coorientador: Prof. Dr. Ronaldo Carlotto Batista

Dissertação de mestrado apresentada ao Instituto de Física da Universidade de São Paulo, como requisito parcial para a obtenção do título de Mestre(a) em Ciências.

Banca Examinadora:
Prof(a). Dr. Edivaldo Moura Santos - Orientador (IF-USP)
Prof(a). Dr(a). Nome do(a) Professor(a) (instituição de trabalho)
Prof(a). Dr(a). Nome do(a) Professor(a) (instituição de trabalho)

São Paulo
2024

FICHA DA BIBLIOTECA

University of São Paulo
Physics Institute

Cosmological Constraints using the Sachs-Wolfe Integrated Effect

Arthur Diniz Meirelles

Supervisor: Prof. Dr. Edivaldo Moura Santos
Co-supervisor: Prof. Dr. Ronaldo Carlotto Batista

Dissertation submitted to the Physics Institute of the University of São Paulo in partial fulfillment of the requirements for the degree of Master of Science.

Examining Committee:
Prof. Dr. Edivaldo Moura Santos - Supervisor (IF-USP)
Prof. Dr. Name (institution)
Prof. Dr. Name (institution)

São Paulo
2024

Frase bonita

Acknowledgements

testando

testando mais

Abstract

ABSTRACT AQUI

Keywords:

Resumo

RESUMO AQUI

Palavras-chave:

List of Figures

List of Tables

Contents

1 | Introduction

The discovery of the Cosmic Microwave Background (CMB) is a fine example of serendipity, Arno A. Penzias and Robert W. Wilson found an unexpected excess temperature while measuring the effective zenith noise temperature in 1964, and after some investigation, they attributed this excess temperature to an isotropic radiation field that today we call the CMB [1]. The CMB has since been used as one of the main probes to studying cosmology, being able to provide various tests and insights into cosmological models [2–4] and measurements of cosmological parameters [5, 6].

In the standard cosmological model, commonly called the ΛCDM model, the CMB is a radiation field that has permeated the universe since the Big Bang, its photons have been freely traveling the universe since their decoupling from electrons and protons during the very early stages of the universe's history [7]. The current measurement for the black body spectrum temperature of the CMB is $2.725\,48(57)\,\mathrm{K}$ [8], and despite being isotropic to many orders of precision, it does contain anisotropies in the order of $10^{-5}\,\mathrm{K}$, which is expected in the ΛCDM model [9]. These fluctuations are the result of many physical effects that contribute to the CMB's emission or are acting on the photons as they travel through the universe, making them an excellent probe to constrain cosmological parameters.

Some mappings of the CMB were carried out in the last few decades, the first satellite launched specifically dedicated to doing this was the Cosmic Background Explorer (COBE) satellite with a 7° angular resolution [10], followed by the Wilkinson Microwave Anisotropy Probe (WMAP) with a 0.3° angular resolution, which was also able to show that CMB photons are polarized, a property related to other physical effects that assisted cosmologists in further understanding the history of the universe[11–13]. In 2009, the Planck Satellite was launched, improving upon WMAP's precision to an impressive value of 5' ($\sim 0.083^\circ$) angular resolution [14], allowing cosmologists to access the finest details in the CMB anisotropies to this day. Figure 1.1 shows a comparison between the resolution of these maps.

Amongst the many effects that affect the CMB, the Integrated Sachs-Wolfe (ISW) Effect is one of the most important ones. First described by Rainer K. Sachs and Arthur M. Wolfe in 1967, the ISW effect is a mechanism that causes photons (including CMB photons) to blueshift

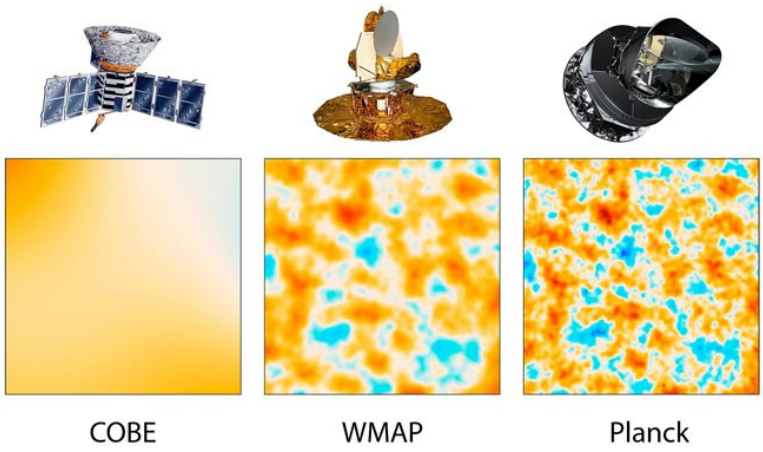

Figure 1.1: Each image represents the same 10 square degree patch of the sky measured by the three telescopes shown above each image, the improvement in the resolution of each map is very noticeable. Credit: NASA/LAMBDA Science Team.

in cosmological periods when gravitational potentials change rapidly. One such period is the time between the current dark energy dominated era and the dark matter dominated era before it. During this transition, gravitational potentials decay (or "flatten") over time, causing CMB photons that entered potential wells with a certain gravitational blueshift to leave these wells with a redshift that does not compensate for the initial blueshift, leaving a net blueshift in these photons, creating patterns that can be observed in the CMB temperature map and spectrum[15].

ILUSTRAÇÃO DO ISW?

There are two contributions to the ISW effect: The early-time ISW effect occurs immediately after the last scattering surface (COMPLEMENTAR AQUI DEPOIS), and the late-time ISW effect, which is more recent, occurring in the current dark energy dominated era.

From this association between blueshifted CMB photons and gravity wells, it is natural to assume that the matter distribution of the universe should hold a statistical cross-correlation between with the CMB temperature map. When looking at the theoretical model, we will see that this cross-correlation is expected, and many works in the past have already searched and found such cross-correlation (EXAMPLE REFS) (COMPLETAR AQUI, VOU COMPLEMENTAR NISSO? APRESENTAR ALGO NOVO? ETC).

The present work expands on a method (what characterizes this method and sets it apart from other ones?) presented in [16] to estimate these cross-correlations, using the models and some techniques presented there, with a more thorough selection of the data that is to be used in

the analysis, using the newer Planck Satellite data instead of the WMAP data, and applying the method to alternative dark energy models, making it possible to compare them with the ΛCDM model and providing insights about the nature of dark energy.

The rest of this dissertation will be organized as follows: DESCRIBE HOW THE SECTIONS ARE ORGANIZED WHEN THE REST OF THE DISSERTATION IS DONE.

2 | Cosmology's Standard Model

The advent of general relativity in the early 20th century allowed physicists to conceptualize mathematical models of the Universe. Albert Einstein proposed a model for a static universe using his theory[17], and other universe models were proposed in the following years. To start this chapter, the fundamental principles of cosmology will be discussed and used to setup a simple background for the universe, and the specificities of the currently most accepted model for the universe – the ΛCDM model – will be discussed. After this, we will complement this simple background with finer details and provide a statistical description of cosmological observables that can be used to test our models.

2.1 The Homogeneous Background

2.1.1 Fundamental Observations and Principles

One of the fundamental principles of cosmology is called the Cosmological Principle: at large scales, the universe is both homogeneous and isotropic. This principle can be used to simplify the description of the energy distribution in the universe, but it also simplifies the possible metrics that can describe the universe to those that have constant curvature (a quantity denoted as k), and it can be shown that any space with constant curvature is locally isometric to: The euclidian plane space ($k = 0$), a hyperspherical space ($k = +1$) or a hyperbolic space ($k = -1$)[18]. The Cosmological Principle has support from a good amount of results in cosmological observations, such as the CMB[10], the galaxy sky distribution[19, 20], amongst others.

In the period from 1927 to 1929, Edwin Hubble and Georges Lemaître, amongst other scientists, greatly contributed to the current understanding of cosmology: Observations were carried out and showed that most galaxies and nebulae data show a redshift proportional to their distances relative to the earth[21], these results were studied using general relativity and cosmological models at the time[22]. It was then established another principle that physicists were avoiding in their theoretical models for quite some time: The universe is not static, in fact it is expanding and there is a linear relationship between the redshift of an observed object and its distance to the observer.

To describe the universe, a coordinate system that can be described using general relativity is embedded in the entire universe, and to describe its dynamical nature, the scale factor a is introduced to the theoretical model: a is set to 1 at the present as a convention (usually called a_0), and its value at any given time $a(t)$ is the size of the universe relative to its present size. A simple relation can be established between the scale factor of an observed object and its redshift z:

$$1 + z = \frac{\lambda_{\text{obs}}}{\lambda_{\text{emit}}} = \frac{a_{\text{obs}}}{a_{\text{emit}}} = \frac{1}{a_{\text{emit}}} \tag{2.1}$$

where λ and a are the wavelength of the radiation and the scale factor, respectively, when emitted (λ_{emit} and a_{emit}) and when observed (λ_{obs} and a_{obs}).

At different times in the universe's history, the scale factor behaves differently, so it is useful to define the Hubble parameter $H(t)$ for a given cosmological time t:

$$H(t) = \frac{1}{a}\frac{\mathrm{d}a}{\mathrm{d}t} \tag{2.2}$$

These properties are not exclusive to any cosmological model, instead being present in most of them. The standard model of cosmology, called the ΛCDM model, usually takes a few assumptions on top of the ones described previously:

- The Universe emerged from a space-time singularity that started expanding many years ago, in an event called the Big Bang;
- Aside from baryonic matter, radiation and neutrinos, there are two other main components in the Universe: Non-relativistic (cold) dark matter and an energy component with constant density called dark energy, which is related to a cosmological constant Λ;
- During the early stages of the Universe's history, it went through a period of rapid acceleration driven by a scalar quantum field.

Based on the Cosmological Principle, most theoretical models first set up a homogeneous and isotropic background description of the universe, and then introduce perturbations to this background, allowing for a detailed statistical description of its evolution. In the rest of this section, we will use the principles and assumptions just presented to set this background.

2.1.2 Friedmann Equations

As already mentioned, the main theoretical framework to describe the universe is the theory of general relativity, since the most relevant force in the scale of the universe is the gravitational force, though in periods close to the Big Bang, other forces need to be taken into account. We then use Einstein's field equations with a cosmological constant Λ:

$$R_{\mu\nu} - \frac{1}{2}g_{\mu\nu}R + \Lambda g_{\mu\nu} = 8\pi G T_{\mu\nu}, \tag{2.3}$$

where $R_{\mu\nu}$ is the Ricci curvature tensor for the universe's metric $g_{\mu\nu}$, R is the Ricci scalar, G is the gravitational constant and $T_{\mu\nu}$ is the energy-momentum tensor.

In equation (2.3) and throughout this text (unless otherwise stated), we will use units such that the Boltzmann constant (k_b), the speed of light in a vacuum (c) and the reduced Planck constant ($\hbar$) are all equal to one. Furthermore, Greek letter tensor indices indicate that the time component of the tensor is included in the equation and Latin letter tensor indices indicate that only spatial components are included. Current results strongly indicate the metric $g_{\mu\nu}$ of the universe to be flat ($k = 0$)[6], thus justifying the use of an Euclidian metric scaled by $a(t)$, and we will assume a homogeneous and isotropic distribution of energy throughout the universe to construct an energy-momentum tensor with constant energy density ρ_0 and constant pressure P[23]:

$$g_{\mu\nu} = \begin{pmatrix} -1 & 0 & 0 & 0 \\ 0 & a^2 & 0 & 0 \\ 0 & 0 & a^2 & 0 \\ 0 & 0 & 0 & a^2 \end{pmatrix} \qquad T_{\mu\nu} = \begin{pmatrix} -\rho_0 & 0 & 0 & 0 \\ 0 & P & 0 & 0 \\ 0 & 0 & P & 0 \\ 0 & 0 & 0 & P \end{pmatrix}. \tag{2.4}$$

The metric $g_{\mu\nu}$ described in equation (2.4) is called the Friedmann-Lemaître-Robertson-Walker (FLRW) metric. In order to expand any equation from (2.3), it's necessary to determine $R = g^{\mu\nu}R_{\mu\nu}$. By expanding the expression using the matrices defined in (2.4), the result is

$$R = 6\left[\frac{\ddot{a}}{a} + \left(\frac{\dot{a}}{a}\right)^2\right]. \tag{2.5}$$

From all the equations in (2.3), if the equation that corresponds to $\mu = \nu = 0$ is expanded

using the result (2.5), one obtains

$$\left(\frac{\dot{a}}{a}\right)^2 = \frac{1}{3}\left(8\pi G\rho_0 + \Lambda\right), \tag{2.6}$$

which relates the relative rate at which the universe is expanding with the energy content of the universe. In the ΛCDM model, Λ is assumed to be the source of the current accelerated expansion of the universe, so an energy component related to this constant is necessary, and it can be defined as

$$\rho_\Lambda = \frac{\Lambda}{8\pi G}, \tag{2.7}$$

such that

$$\left(\frac{\dot{a}}{a}\right)^2 = \frac{8\pi G}{3}\rho, \tag{2.8}$$

where $\rho = \rho_\Lambda + \rho_0$. This is called Friedmann's first equation.

When any of the space-space equations of (2.3) is expanded and the resulting equation is combined with equation (2.8), Friedmann's second equation is obtained:

$$\frac{\ddot{a}}{a} = -\frac{4\pi G}{3}(\rho + 3P). \tag{2.9}$$

This equation is a relation between the acceleration of the universe and its energy content, it's clear that $P < -\frac{1}{3}\rho$ indicates a universe expanding with a positive acceleration, which is highly unexpected since gravity is an attractive force, but in section 2.1.3 the case of the cosmological constant will be discussed, in which Λ yields $P_\Lambda = -\rho_\Lambda$, being the reason it contributes to an accelerated expansion.

2.1.3 Energy Content

To understand the contribution of each component of the universe to its dynamics, a differential equation for each component has to be determined, we do this using the energy-momentum conservation equation:

$$\nabla_\mu T^\mu_\nu \equiv \partial_\mu T^\mu_\nu + \Gamma^\mu_{\alpha\mu} T^\alpha_\nu - \Gamma^\alpha_{\nu\mu} T^\mu_\alpha = 0. \tag{2.10}$$

Again using the energy-momentum tensor defined in (2.4), the following equation is obtained:

$$\frac{\partial \rho}{\partial t} + \frac{\dot{a}}{a}(3\rho + 3P) = 0. \tag{2.11}$$

To solve this, a relation between density and pressure for each component of the universe is needed, an equation of state. It is commonly assumed that, for a given component s of the universe, its equation of state takes the form

$$P_s = w_s \rho_s, \tag{2.12}$$

where w_s is called the equation of state parameter. Using that equation and solving for $\rho_s(a)$ on equation (2.11) yields

$$\rho_s(a) \propto \exp\left[-3\int_1^a \frac{da'}{a'}[1 + w_s(a')]\right]. \tag{2.13}$$

This solution ignores further interaction between components, it would apply to a single-component universe, but it is also a useful first approximation in epochs of dominance of a single component. In the ΛCDM model, it is assumed that all components of the universe possess a constant value for w_s, in that case the solution is simple:

$$\rho_s(a) \propto a^{-3(1+w_s)}. \tag{2.14}$$

This represents the evolution of the density parameter of any component as a function of the scale parameter, and thus as a function of cosmological time, since $a(t)$ is monotonically increasing (the universe has not reduced at any point in its history so far).

The rigorous form of determining w_s for some components of the universe requires the usage of statistical physics, assuming distribution functions and using the Boltzmann equation to determine these values. In cases where we have limited information on the physical properties of a certain component, such as dark energy, theoretical frameworks and assumptions have to be used, as well as the analysis of data.

In the case of dark energy, assuming its origin is related to the cosmological constant, the data strongly suggests a value of $w_\Lambda = -1$, which also indicates a constant density for dark energy, being a simple model in the scope of cosmology and data analysis, but this result has

no consistent theoretical estimation. Many models propose alternative possibilities, such as dynamical dark energy in which w_{DE} is a function of a[24], which would still be able to explain the accelerated expansion of the universe as long as $w_{DE} < -\frac{1}{3}$. Table 2.1 summarizes the equation of state properties of each known component in the universe.

It is very useful to also define the energy density fraction of each component of the universe using

$$\Omega_s = \frac{\rho_s(a_0)}{\rho_{\text{crit}}}, \tag{2.15}$$

where ρ_{crit} is the so called critical density, defined as

$$\rho_{\text{crit}} \equiv \frac{3H_0^2}{8\pi G}, \tag{2.16}$$

where H_0 is the Hubble constant, the value of the Hubble parameter $H(t)$ defined in (2.2) at the present.

This energy density makes it possible to determine what is the curvature of the universe: If the total sum of energy densities in the universe is equal to the critical density, the universe is flat; if this sum is higher than ρ_{crit} the universe would have positive curvature; and if this sum is lower than ρ_{crit}, the universe would have negative curvature.

Table 2.1 summarizes the current estimated values for these energy fractions for the universe in the present. It is important to note that commonly in cosmology (and throughout this text), the classification of baryons includes electrons, even though they are classified as leptons.

Component	$\rho(a)$	w	Ω
Baryonic matter	$\rho_0 a^{-3}$	0	0.05
Cold dark matter	$\rho_0 a^{-3}$	0	0.26
Radiation	$\rho_0 a^{-4}$	$\frac{1}{3}$	5×10^{-5}
Dark energy	ρ_0	-1	0.68
Curvature	$\rho_0 a^{-2}$	$-\frac{1}{3}$	0.001

Table 2.1: Equation of state parameters w, energy density functions $\rho(a)$ and energy density fractions for each known component of the universe according to the ΛCDM model. Most data were adapted from Planck[6], the radiation data was taken from `https://ned.ipac.caltech.edu/level5/March04/Lahav/Lahav1_4.html`.

2.1.4 Dark Energy Models

Many approaches to study dark energy have been proposed, each of them with different properties, ranging from parameterization of the equation of state[25, 26] to alternative fluid models for dark energy[27] and modifications to general relativity[28].

The simplest parametrization proposed for dark energy's equation of state is called the Chevallier-Polarski-Linder (CPL) parametrization:

$$w(z) = w_0 + \left(1 - \frac{1}{1+z}\right) w_a. \tag{2.17}$$

One important property of this parametrization and most others is that the value of the equation of state parameter today ($z = 0$) is a constant term of the equation that can be used as a free parameter during data analysis.

So far, this parametrization has not solved some of the current limitations being faced by the ΛCDM model, such as the Hubble tension [29] and the σ_8 tension [6], it has not improved over the ΛCDM predictions, but it shows good compatibility with CMB, type 1A supernovae and baryon acoustic oscillations (BAO) data[6]. Planck results using this parametrization are shown in Table 2.2.

Parameter	Marginalized Value
w_0	-0.957 ± 0.080
w_a	$-0.29^{+0.32}_{-0.26}$
H_0[km s^{-1}Mpc^{-1}]	68.31 ± 0.82
σ_8	0.820 ± 0.011
$\Delta\chi^2$	-1.4

Table 2.2: Marginalized values and 68% confidence limits for cosmological parameters, assuming parametrization (2.17), obtained by combining Planck temperature and polarization autocorrelation and cross-correlation spectra[30], type 1A supernovae data from the Joint Light Curve Analysis (JLA)[31] and BAO data from the Sloan Digital Sky Survey (SDSS)[32]. The $\Delta\chi^2$ value was computed with respect to the ΛCDM best fits computed from the same data set combination.

2.1.5 A Brief History of the Universe

There are many details and equations that are used to describe the universe, and we commonly categorize many stages of the universe according to important events that happened during its

history. The ΛCDM model assumes the universe started as a singularity; as it started expanding, quantum fluctuations at that time would eventually result in inhomogeneities thought to be the source for the formation of structure in the universe.

The next important period of the universe's evolution was a highly accelerated expansion epoch driven by an effect called cosmic inflation, first proposed as a solution to the horizon problem[33, 34], a problem that questioned how can the CMB temperature differences across the sky be so small ($\sim 10^{-5}$ K), even between points apparently causally disconnected during all epochs of the universe's thermal history. The ΛCDM model assumes inflation was driven by a quantum scalar field[23]. Definitive evidence of the inflation model may be reached with the detection of a certain type of polarization of the CMB called the B-modes, which have not been detected yet, but have reached good constraints.[13]

Briefly after inflation, baryons and photons are still coupled through Compton scattering, thus photons are still unable to travel freely, the Universe at this point is composed of photons coupled with baryons, helium nuclei, and trace amounts of Lithium. With the decrease in temperature, hydrogen atoms can form without being quickly ionized, Compton scattering eventually can no longer maintain baryons and photons coupled, resulting in a decoupling of these components. The photons are released to travel across the Universe, the radiation field formed from this period is what we currently measure as the CMB.

After this, an epoch called "the Dark Ages" starts, most of the photons in the universe are the result of the decoupling described before and stars are yet to be formed, which is the reason why it is called a dark age. Matter dominates this period and many to follow, greatly decreasing the rate of expansion of the universe. As a result of the quantum fluctuations in the early universe, stars, galaxies, and other structures form. The study of the formation of structure is completely dependent on the study of the inhomogeneous aspect of the universe, for which some of the detailed theoretical framework will be covered in the next section.

Figure 2.1 shows a summarized and visual representation of some of the events described in this section.

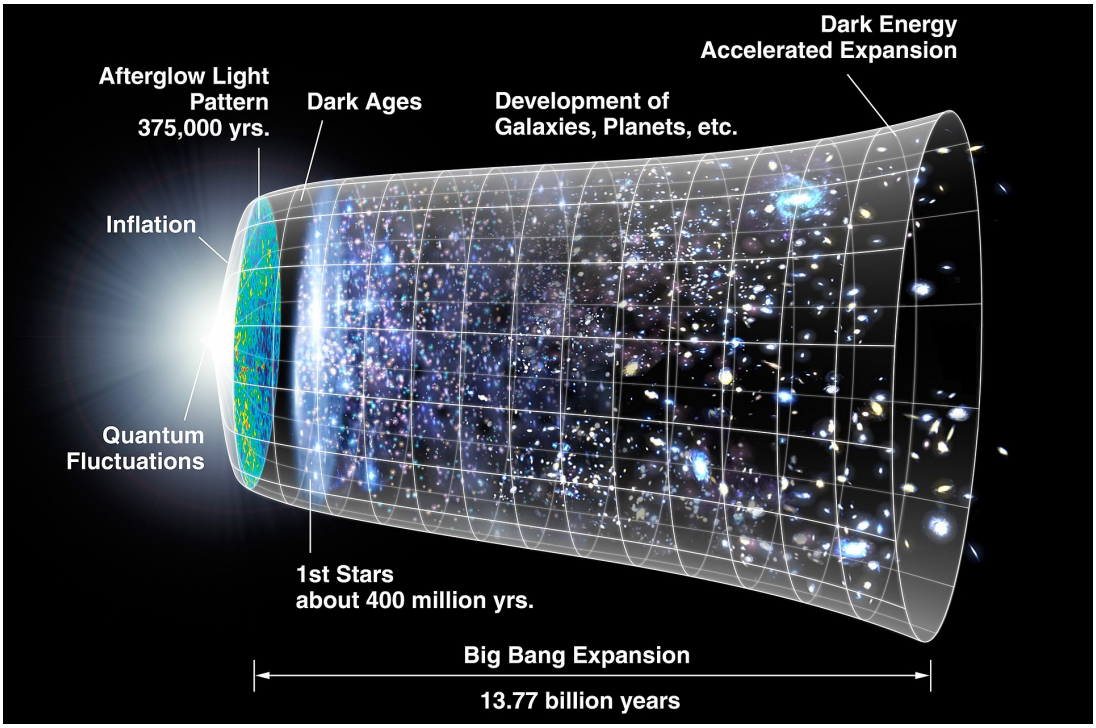

Figure 2.1: A representation of the time evolution of the universe, starting from the left (the Big Bang) with time passing towards the right. The radius of each section indicates the size of the universe at that time; during inflation this radius increases very rapidly, indicating an accelerated expansion during this period, while closer to the present the slope of increase in size shows a slight acceleration, indicating the current dark energy accelerated period. Briefly after the inflation period (in cosmological time), the photons decouple from baryons, leaving a radiation field in the universe, resulting in the CMB, represented in the image by the afterglow of inflation. After this, the only radiation in the universe is this afterglow for many years, during that time structure starts to form from the small inhomogeneities left by quantum fluctuations in the very early stages of the universe, forming the first stars and then the first galaxies. Credit: NASA/WMAP Science Team.

2.2 Inhomogeneities and Anisotropies

The existence of structure – nebulae, stars, galaxies, clusters – in the Universe indicates that, throughout its history, it has been inhomogeneous and anisotropic at some scale, these perturbations to the uniform background are relatively small though, take the CMB for instance: CMB anisotropies are around 5 orders of magnitude lower than its average black body temperature[5].

In this scenario, there is no known theoretical model that can predict the exact behavior of every particle in the universe, instead we turn to a statistical prediction taking into account the properties of space-time and the components of the universe. In this section, the first order equations that govern these properties will be shown by introducing perturbations both to the

metric and to the stress-energy tensor.

2.2.1 Perturbed Space-Time

In the ΛCDM model, to account for perturbations in the uniform background previously set, we use the following new form for the metric:

$$\begin{cases} g_{00} = -1 - 2\Psi(\mathbf{x}, t), \\ g_{0i} = g_{i0} = 0, \\ g_{ij} = a^2(t)\delta_{ij}[1 + 2\Phi(\mathbf{x}, t)]. \end{cases} \tag{2.18}$$

With the use of the geodesic equation on this new tensor and using a first order approximation, it's possible to obtain the following results for the motion equations of particles traveling through this perturbed space-time:

$$\frac{\mathrm{d}x^i}{\mathrm{d}t} = \frac{\hat{p}_i}{a}\frac{p}{E}(1 - \Phi + \Psi), \tag{2.19}$$

$$\frac{\mathrm{d}p^i}{\mathrm{d}t} = -(H + \dot{\Phi})p^i - \frac{E}{a}\partial_i\Psi - \frac{1}{a}\frac{\mathrm{d}p^i}{\mathrm{d}E}p^k\partial_k\Phi + \frac{p^2}{aE}\partial_i\Phi. \tag{2.20}$$

We can use

$$\frac{\mathrm{d}p}{\mathrm{d}t} = \frac{\mathrm{d}}{\mathrm{d}t}\sqrt{\delta_{ij}p^ip^j} = \delta_{ij}\frac{p^i}{p}\frac{\mathrm{d}p^j}{\mathrm{d}t} \tag{2.21}$$

and $\hat{p}^i = p^i/p$ in combination with equation (2.20) to find separate equations for p and $\hat{p}^i$:

$$\frac{\mathrm{d}p}{\mathrm{d}t} = -[H + \dot{\Phi}]p - \frac{E}{a}\hat{p}^i\partial_i\Psi, \tag{2.22}$$

$$\frac{\mathrm{d}\hat{p}^i}{\mathrm{d}t} = \frac{E}{ap}[\delta^{ik} - \hat{p}^i\hat{p}^k]\partial_k\left(\frac{p^2}{E^2}\Phi - \Psi\right). \tag{2.23}$$

As for the dynamics of the field perturbations, it's possible to use Einstein's field equations to obtain, in Fourier space (see Appendix A), the equations for scalar perturbations on the gravitational potentials[23]

$$k^2\Phi + 3H(\dot{\Phi} - H\Psi) = -4\pi Ga^2(\rho_{DM}\delta_{DM} + \rho_b\delta_b + 4\rho_\gamma\Theta_0 + 4\rho_\nu\mathcal{N}_0), \tag{2.24}$$

$$k^2(\Phi + \Psi) = -32\pi G a^2(\rho_\gamma \Theta_2 + \rho_\nu \mathcal{N}_2). \tag{2.25}$$

Here, the terms Θ_0, Θ_2, $\mathcal{N}_0$ and $\mathcal{N}_2$ are obtained in the calculation of the perturbed energy-momentum tensor, they are defined as

$$F_\ell = \frac{1}{(-i)^\ell} \int_{-1}^{1} \frac{\mathcal{P}_\ell(\mu) F(\mu)}{2} d\mu, \tag{2.26}$$

where F can either represent Θ or $\mathcal{N}$; $\mu = \hat{k} \cdot \hat{p}$ is the cosine between the momentum direction of the photon and the Fourier space wavevector; P_ℓ are Legendre polynomials; the functions $\Theta(\mu)$ and $\mathcal{N}(\mu)$ are the distributions of photon and neutrino perturbations; and i is the imaginary unit $i^2 = -1$.

2.2.2 The Boltzmann Equation

The Boltzmann equation is a fundamental component in the study of every component of the universe. One general form of writing the Boltzmann equation is

$$\frac{\mathrm{d}f}{\mathrm{d}t} = \frac{\partial f}{\partial t} + \frac{\partial f}{\partial x^i} \cdot \frac{\mathrm{d}x^i}{\mathrm{d}t} + \frac{\partial f}{\partial p} \frac{\mathrm{d}p}{\mathrm{d}t} + \frac{\partial f}{\partial \hat{p}^i} \cdot \frac{\mathrm{d}\hat{p}^i}{\mathrm{d}t} = C[f], \tag{2.27}$$

where f is the distribution function of the component to be analyzed and $C[f]$ is the collision term, a factor that is calculated by considering the interactions of such components.

Using equations (2.22) and (2.23) with the Boltzmann equation and assuming $E = p$, i.e. assuming a relativistic particle such as photons, the full first order Boltzmann equation for photons is

$$\begin{aligned} \frac{\mathrm{d}f}{\mathrm{d}t} =& \frac{\partial f}{\partial t} + \frac{\partial f}{\partial x^i} \frac{\hat{p}^i}{a}(1 - \Phi - \Psi) - \frac{\partial f}{\partial p} \left\{ [H + \dot{\Phi}]p + \frac{1}{a} p^i \partial_i \Psi \right\} \\ &+ \frac{\partial f}{\partial \hat{p}^i} \frac{1}{a} \left[\partial_i(\Phi - \Psi) - \hat{p}^i \hat{-}^k \partial_k(\Phi - \Psi) \right]. \end{aligned} \tag{2.28}$$

The first order approximation is being used, and so it is possible to simplify this expression further. For instance, the distribution f for the homogeneous background takes the form of Bose-Einstein's distribution, which means there is no dependence on $\hat{p}^i$ and x^i in this case. It's commonly assumed that the deviations from this distribution are of the same order of the perturbations Φ and Ψ, so both $\frac{\partial f}{\partial x^i}$ and $\frac{\partial f}{\partial \hat{p}^i}$ are first order factors, multiplied by Φ or Ψ result in

second order terms which can be neglected, resulting in

$$\frac{\mathrm{d}f}{\mathrm{d}t} = \frac{\partial f}{\partial t} + \frac{\hat{p}^i}{a}\frac{\partial f}{\partial x^i} - \left[H + \dot{\Phi} + \frac{1}{a}\hat{p}^i\partial_i\Psi\right] p\frac{\partial f}{\partial p}. \tag{2.29}$$

This is an important equation for the description of the CMB, but the description of anisotropies for massive particles is still important, for which the same assumptions are made, resulting in

$$\frac{\mathrm{d}f}{\mathrm{d}t} = \frac{\partial f}{\partial t} + \frac{p}{Ea}\hat{p}^i\frac{\partial f}{\partial x^i} - \left[H + \dot{\Phi} + \frac{E}{ap}\hat{p}^i\partial_i\Psi\right] p\frac{\partial f}{\partial p}. \tag{2.30}$$

The only difference between these equations is the term E/p which, in the case of radiation, is equal to 1. The first order approximation for non-relativistic matter breaks down in the late universe, a non-linear model is necessary in this scenario.

To arrive at a differential equation from this, a function to describe the perturbations needs to be defined, and so does the distribution function. Taking the CMB as an example, the perturbed form of the temperature distribution for CMB photons in general can be defined as

$$T(\mathbf{x}, \hat{\mathbf{p}}, t) = \bar{T}(t)[1 + \Theta(\mathbf{x}, \hat{\mathbf{p}}, t)], \tag{2.31}$$

where $\bar{T}$ is the average temperature in a given time and Θ is a dimensionless field that quantifies the perturbations of the CMB distribution with respect to its average value. This perturbation field can be expressed in terms of the set of functions Θ_ℓ defined in (2.26) by the following equation in Fourier space:

$$\Theta(\hat{\mathbf{k}}, \mu) = \sum_{\ell=0}^{\infty}(2\ell + 1)(-i)^\ell\Theta_\ell(\hat{\mathbf{k}})\mathcal{P}_\ell(\mu). \tag{2.32}$$

If we use the Bose-Einstein distribution for the temperature defined in (2.31) and expand it to its first order, we obtain

$$f(\mathbf{x}, \mathbf{p}, t) = f^{(0)}(p, t) - p\frac{\partial f^{(0)}(p, t)}{\partial p}\Theta(\mathbf{x}, \mathbf{p}, t), \tag{2.33}$$

where

$$f^{(0)}(p,t) = \left[\exp\left(\frac{p}{\bar{T}}\right) - 1\right]^{-1} \tag{2.34}$$

We can then expand the Boltzmann equation using the results in (2.33) and (2.34) and take into account Compton scattering to calculate the collision term $C[f]$ to obtain a differential equation for the CMB photons. We can use similar procedures, using adequate distribution functions, and obtain a set of coupled differential equations to describe the evolution of the perturbations of every known component of the universe in Fourier space[23]:

$$\dot{\Theta} + ik\mu\Theta = -\dot{\Phi} - ik\mu\Psi - \dot{\tau}\left[\Theta_0 - \Theta + \mu v_b - \frac{1}{2}\mathcal{P}_2(\mu)(\Theta_2 + \Theta_{P2} + \Theta_{P0})\right], \tag{2.35}$$

$$\dot{\Theta}_P + ik\mu\Theta_P = -\dot{\tau}\left\{-\Theta_P + \frac{1}{2}[1 - \mathcal{P}_2(\mu)](\Theta_2 + \Theta_{P2} + \Theta_{P0})\right\}, \tag{2.36}$$

$$\dot{\delta} + ikv = -3\dot{\Phi}, \tag{2.37}$$

$$\dot{v} + Hv = -ik\Psi, \tag{2.38}$$

$$\dot{v_b} + Hv_b = -ik\Psi + \frac{4\rho_\gamma}{3\rho_b}\dot{\tau}(v_b + 3i\Theta_1), \tag{2.39}$$

$$\dot{\mathcal{N}} + ik\mu\mathcal{N} = -\dot{\Phi} - ik\mu\Psi. \tag{2.40}$$

Here, Θ_P is the polarization field and $\Theta_{P\ell}$ is defined by equation (2.26) using $F = \Theta_P$; δ and δ_b are the perturbations to the matter and baryon distributions respectively; v and v_b are the bulk velocities of the fluids in the stress-energy tensor for matter and baryons respectively; ρ_b and ρ_γ are the baryon and radiation energy densities respectively; and τ is the optical depth of the universe.

These equations, alongside equations (2.24) and (2.25), are very complex to be solved analytically, so it is common to evolve them numerically, and there are a few codes developed specifically to do this. One of them, that has been used in this project, is CAMB.[35, 36]

2.3 The Cosmic Microwave Background

With the dynamical equations for photons determined, one can obtain the temperature perturbation distribution Θ if initial conditions are provided. With the equations already presented,

it is possible to show that the initial conditions at the early universe depend only on the initial conditions for Φ[23], these conditions are then evolved through the inflationary period, which assumes the existence of a quantum scalar field $\phi(\mathbf{x}, t)$ that drives a brief accelerated expansion.

At this point, baryons have formed and the photons are tightly coupled to them, forming a baryon-photon fluid that can be described by the differential equations (2.35) - (2.40), the initial distribution obtained for this fluid can then be used as the initial condition and evolved to predict the present anisotropies to the uniform background. To analyze these predictions, the statistical behavior of each component of the universe is taken: either their spectral densities (see Appendix A) – usually called their power spectra – or what is known as their correlation spectra.

2.3.1 CMB Autocorrelation Spectrum

Equation (2.31) explicitly assumes a dependence in position, time, and momentum direction, measurements made on Earth can assume a fixed value for time since our measurements related to the universe are taken in a period negligible in the cosmological scale, but the translational movement of the Earth is relevant to our measurements: measurements of the CMB over a time period made by a non-comoving observer, when projected onto a sphere, lead to a strong dipole pattern in the temperature distribution, modulation of the multipole terms of this temperature distribution and a small relativistic aberration [37–39].

Despite these effects, measurements of this temperature distribution can be projected onto a sphere independent of the Earth's position, with corrections taking these effects into account, making it possible to describe this distribution simply using two angle variables, or simply $\hat{\mathbf{p}}$.

We can expand the temperature perturbations in spherical harmonics:

$$\Theta(\mathbf{x}, \hat{\mathbf{p}}, t) = \sum_{\ell=1}^{\infty} \sum_{m=-\ell}^{\ell} a_{\ell m}(\mathbf{x}, t) Y_{\ell m}(\hat{\mathbf{p}}). \tag{2.41}$$

All the information about temperature maps of the CMB measured on Earth are contained in the set of $a_{\ell m}$ values. Given the limited number of pixels N_{pix} of any of these maps, there is a maximum value of ℓ (ℓ_{max}) beyond which very little additional information would be obtained. For each value of ℓ, there are $2\ell + 1$ values of m – and $a_{\ell m}$ – in the series, a hypothetical observed map with precision p_r in squared radians would have $4\pi/p_r$ pixels, setting this number of pixels equal to the number of $a_{\ell m}$ used to describe this map gives a reasonable estimation of ℓ_{max}[23],

so

$$\sum_{\ell=0}^{\ell=\ell_{\text{max}}} (2\ell+1) = (\ell_{\text{max}}+1)^2 = N_{\text{pix}} = \frac{4\pi}{p_r}. \tag{2.42}$$

Using the orthogonality property of the spherical harmonics, one can obtain a direct expression for $a_{\ell m}$ in terms of the angular distribution of the perturbations:

$$a_{\ell m}(\mathbf{x}, t) = \int \frac{d^3k}{(2\pi)^3} e^{i\mathbf{k}\cdot\mathbf{x}} \int d\Omega Y^*_{\ell m}(\hat{\mathbf{p}})\Theta(\mathbf{k}, \hat{\mathbf{p}}, t). \tag{2.43}$$

Again, there are available codes that efficiently and precisely calculate $a_{\ell m}$ from a pixelized map and vice versa, the one used in this work was HEALPix[40]. Under the hypothesis that the spherical harmonics coefficients $a_{\ell m}$ are independent Gaussian random variables with zero mean, all its statistical properties are contained in the variance C_ℓ, also known as the power spectrum:

$$\langle a_{\ell m} a^*_{\ell' m'} \rangle = \delta_{\ell\ell'}\delta_{mm'}C(\ell), \tag{2.44}$$

where $\delta_{mm'}$ is the Kronecker delta taking m and m' as arguments.

The fact that for lower values of ℓ there are fewer coefficients $a_{\ell m}$ naturally leads to lower multipoles ℓ having higher uncertainty, this property is usually called cosmic variance and can be expressed using[23]

$$\left(\frac{\Delta C(\ell)}{C(\ell)}\right)_{\text{cosmic variance}} = \sqrt{\frac{2}{2\ell+1}}. \tag{2.45}$$

The temperature autocorrelation defined in equation (2.44) is usually expressed as C_ℓ^{TT}, but sometimes a modified spectrum $D_\ell^{TT} = \frac{\ell(\ell+1)}{2\pi}C_\ell^{TT}$ is used for visualization purposes. Figure 2.2 shows Planck's CMB power spectrum data and its corresponding best-fit spectrum assuming a ΛCDM cosmology.

2.3.2 Analytical Approximation

Although solving equations such as (2.35) numerically gives accurate results, obtaining an analytical approximation to these equations helps us understand the underlying physical effects that most influence the evolution of the perturbations. Assuming a small dependency

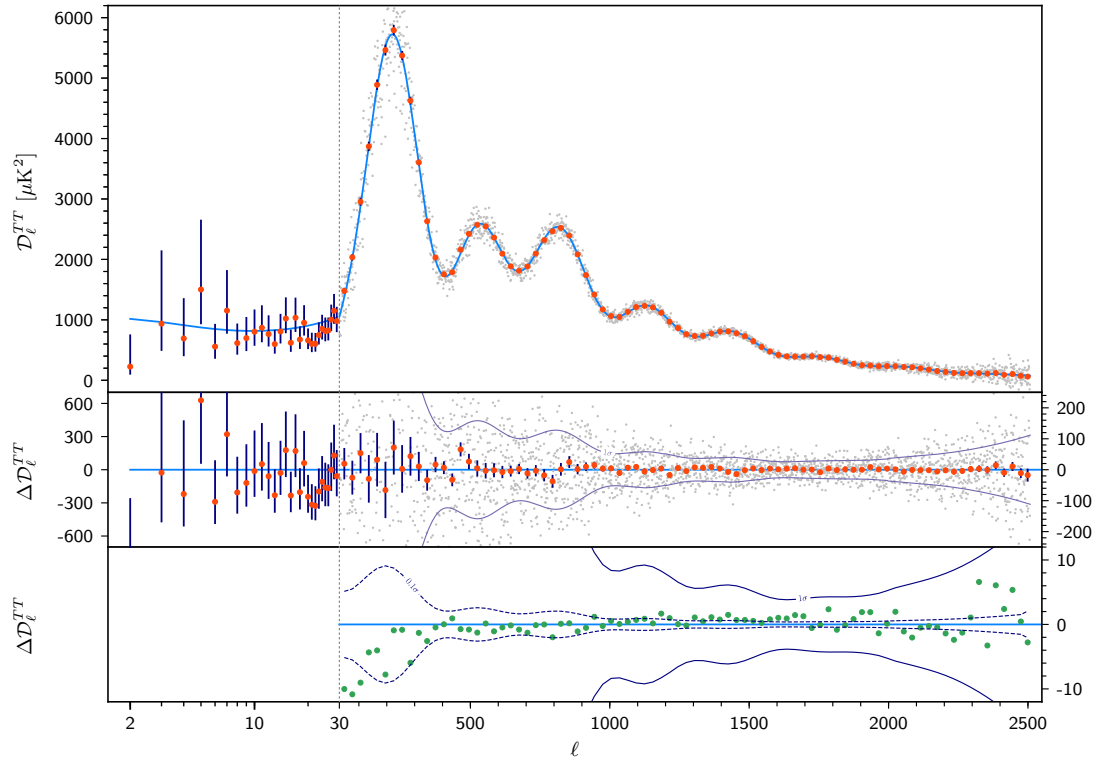

Figure 2.2: Planck 2018 CMB temperature power spectrum: the blue line corresponds to a ΛCDM cosmology best-fit to the data points in orange. For $\ell < 30$ a logarithmic scale was used and the data points correspond to the D_ℓ^{TT} for each value of ℓ, while for $\ell \geq 30$ a linear scale was used and the data points correspond to binned values for the data for D_ℓ^{TT}, which are represented as gray dots. The error bars show $\pm 1\sigma$ uncertainties, including cosmic variance. The middle panel shows the 1σ lines for the unbinned data points, while the bottom panel shows the difference between the 2015 and 2018 coadded high-multipole spectra (green points). Extracted from [30].

on polarization and taking the recombination to be instantaneous, one can obtain the following equation[23]:

$$\begin{aligned}\Theta_\ell(k,\eta_0) \approx &[\Theta_0(k,\eta_*) + \Psi(k,\eta_*)]j_\ell[k(\eta_0-\eta_*)] \\ &+ 3\Theta_1(k,\eta_*)\left\{j_\ell[k(\eta_0-\eta_*)] - (l+1)\frac{j_\ell[k(\eta_0-\eta_*)]}{k(\eta_0-\eta_*)}\right\} \\ &+ \int_0^{\eta_0} d\eta e^{-\tau}[\Psi'(k,\eta) - \Phi'(k,\eta)]j_\ell[k(\eta_0-\eta)],\end{aligned} \tag{2.46}$$

where j_ℓ are spherical Bessel functions, η is the conformal time

$$\eta = \int_0^t \frac{dt}{a(t)}, \tag{2.47}$$

and η_* is the value of η that maximizes the visibility function $g(\eta)$:

$$g(\eta) = -\tau' e^{-\tau}. \tag{2.48}$$

With these conventions, the derivative with respect to η is being represented by the apostrophe notation, while the dot notation used in equation (2.35) will still indicate derivatives with respect to time.

There are three main contributors to the solution (2.46):

- The $(\Theta_0 + \Psi)$ term is usually called the Sachs-Wolfe term, which is associated with Baryon Acoustic Oscillations (BAO), which are fluctuations in the density of the visible baryonic matter of the universe, caused by acoustic density waves in the primordial plasma of the early universe[23];
- The $3\Theta_1$ term shows the same acoustic oscillations out of phase due to a Doppler shift;
- The last term, an integral involving the time variations of the gravitational potentials, represents the Integrated Sachs-Wolfe (ISW) effect. Its dependence on the variation of the gravitational potential makes it so that it only has a non-negligible effect on the CMB at cosmological periods with high variation of these potentials: At around $a \approx 10^{-4}$ the Universe transitioned from a radiation-dominated to a matter-dominated universe (early ISW), and recently – around $a \approx 0.61$ or $z \approx 0.63$[41] according to the ΛCDM model – the universe transitioned from a matter-dominated universe to the current dark energy dominated universe (late ISW).

With this in mind, we can use only the ISW term in the temperature perturbations to estimate its contribution to the CMB autocorrelation spectrum and use the results as a probe of the ISW effect. Figure 2.3 shows a comparison of the late-ISW contribution to the CMB spectrum compared to its full calculation in the large scale (low multipole) terms.

We can also go further, and analyze the contribution of this term to other types of spectra, such as the matter contrast distribution spectrum and do the same. In section 2.4 we will determine the final theoretical predictions for the ISW effect's contribution to three types of spectra and discuss their uses as probes of this effect. Later, in chapter 3, we will discuss how to draw these

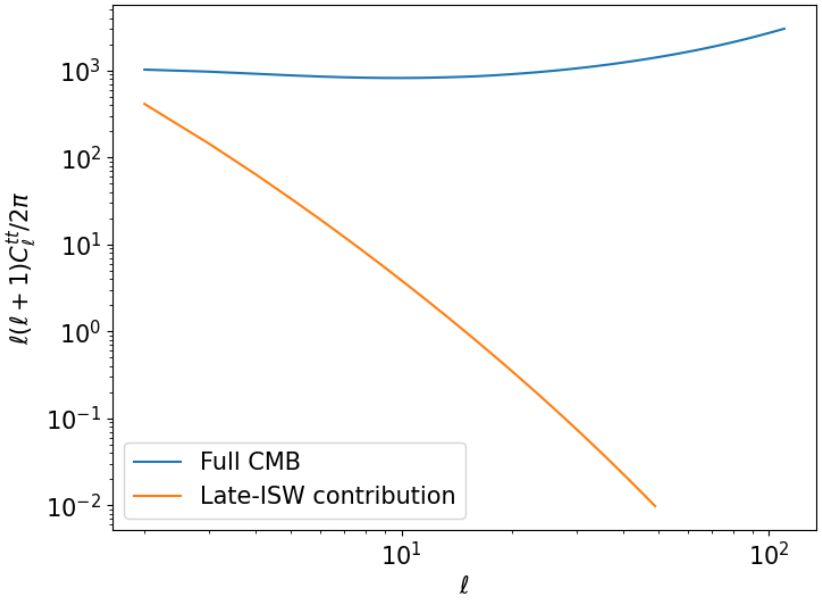

Figure 2.3: CMB autocorrelation comparison for the late-ISW term and the full spectrum. Calculations were made using CAMB (for the full spectrum) and codes developed during the project. The parameters used are those corresponding to the Planck best fit parameters[6].

spectra from cosmological data, which can be compared with the theoretical predictions in order to determine cosmological constraints, including constraints related to dark energy.

2.4 The Integrated Sachs Wolfe Effect

It was proposed that the cross-correlation spectrum between CMB maps and matter contrast could be used to detect the ISW effect[42], and since then many works have reported the detection of this signal[43–46]. In this section, a framework for theoretical estimations of the ISW contribution to this cross-correlation will be discussed.

2.4.1 The Matter Power Spectrum

To study the distribution of matter we observe, there is a difference compared to the CMB: While the CMB is usually described as a two dimensional map measured around the Earth, the matter distribution in the universe is first analyzed taking the distance from the Earth into consideration, so three coordinates are necessary, and then one can take a 2D projection for a

certain redshift z. Again using Fourier space, we first define the 3D matter power spectrum for the distribution of matter perturbations in the universe $P(k)$ as

$$\langle \delta(\mathbf{k}, z)\delta^*(\mathbf{k}', z)\rangle = (2\pi)^3 P(k, z)\delta_D(\mathbf{k} - \mathbf{k}'), \tag{2.49}$$

where δ_D is the Dirac delta, δ is the previously shown matter perturbation distribution in the universe and the $*$ superscript indicates the complex conjugate of a quantity. Again, using appropriate initial conditions, one can determine $\delta(\mathbf{k})$ and thus $P(k, z)$, and again these results can be obtained numerically using CAMB, Figure 2.4 shows the results for this calculation using the Halofit model[47], a semi-analytical method to determine a non-linear solution for $P(k, z)$.

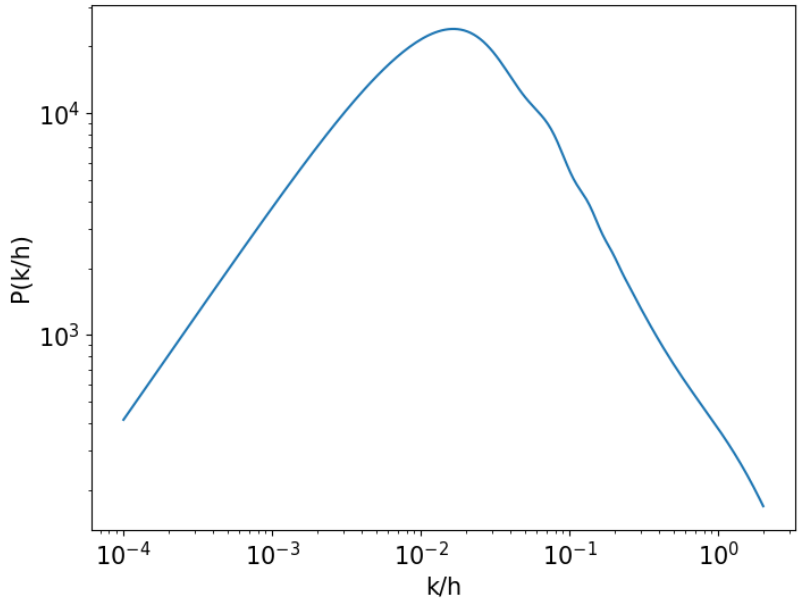

Figure 2.4: Matter power spectrum calculated as a function of k/h, where $h = H_0/100$ using the Halofit with cosmological parameters according to Planck's best fit results[6].

The dependence of the ISW effect on the matter distribution makes it so that this power spectrum is necessary for calculations regarding the influence of the ISW effect on certain observables.

2.4.2 The Galaxy-CMB Correlation Spectra

One can follow a similar process to the one presented for the CMB to obtain the autocorrelation for a spherical projection of a matter density distribution on a spherical shell on a certain

redshift z, but to do that in a way that can be compared with cosmological data, one has to choose a way to trace the matter density with an observable. One way of doing this is by tracing the mass distribution with galaxy density on a certain redshift, it is common to assume the density contrast of galaxy density takes the form $\delta_g = b_g\delta$ where b_g is a constant value (for each redshift z) called the bias factor. From this point, the same process would apply: Expand the distribution in spherical harmonics with factors $a^g_{\ell m}$ and calculate the variance of these variables to obtain an autocorrelation spectrum $C^{gg}(\ell)$.

Similarly, instead of calculating an autocorrelation spectrum, one can calculate a cross-correlation between two perturbation distributions, which is analogous to definition (2.44):

$$\left\langle a^t_{\ell m} a^g_{\ell' m'} \right\rangle = C^{tg}(\ell)\delta_{\ell\ell'}\delta_{mm'}. \tag{2.50}$$

For simplicity and computational purposes, one can determine a general equation to calculate these spectra, and taking this one step further, one can calculate the perturbations only due to ISW effect using only its term in equation (2.46) and determine a formula that calculates its contribution to any spectra. In this work we have used the form shown in [16]:

$$C^{xy}_\ell = \frac{2}{\pi}\int dk k^2 W^x_\ell(k) W^y_\ell(k) P(k), \tag{2.51}$$

where x and y can represent g or t, and W_ℓ are called the kernel functions, which can be calculated using

$$W^t_\ell = -3\Omega_m \left(\frac{H_0}{k}\right)^2 \int dz \frac{\mathrm{d}[(1+z)D(z)]}{\mathrm{d}z} j_\ell[k\chi(z)], \tag{2.52}$$

$$W^g_\ell = \int dz b_g(z) \frac{\mathrm{d}N}{\mathrm{d}z} D(z) j_\ell[k\chi(z)], \tag{2.53}$$

where $D(z)$ is the linear growth function (normalized to 1 at $z = 0$); $\chi(z)$ is the comoving distance; and $\frac{\mathrm{d}N}{\mathrm{d}z}$ is the normalized galaxy redshift distribution, also called the selection function[43].

With equation (2.51), we can determine the theoretical spectra for CMB and galaxy auto-correlations and CMB-galaxy cross-correlation directly. Figure 2.5 shows examples of these correlation spectra for all three possible combinations, calculated numerically.

These plots, alongside 2.3, show very clearly that the ISW effect has a lot more relevance in

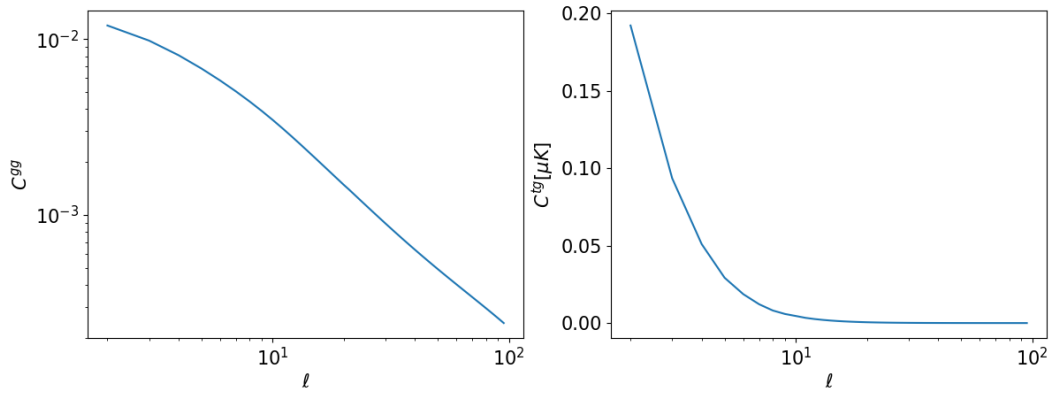

Figure 2.5: Galaxy autocorrelation spectrum (left) and late-ISW contribution to the galaxy-CMB cross-correlation (right). The selection function used to calculate these spectra was parametrized to be compatible with 2MASS' galaxy redshift distribution[16, 48].

the lower multipoles, where cosmic variance has a significant influence. The selection function is an important aspect of this signal, in chapter 4 the matter of how to optimize the signal with the use of an idealized selection function will be discussed.

3 | Extracting Correlations from Data

4 | Results

5 | Conclusions

Artigo do Edivaldo: [16]

ISW artigo original: [15]

The GNU parallel software was used: [49]

Cobaya: [50, 51]

Gibbs Sampling: [52]

Appendices

A | Fourier Space

Falar sobre espaço de fourier

Falar do conceito de spectral density/power spectrum

B | Monte Carlo Markov Chains

Bibliography

[1] A. A. Penzias and R. W. Wilson. "A Measurement of Excess Antenna Temperature at 4080 Mc/s." In: *Astrophysical Journal* 142 (July 1965), pp. 419–421. DOI: 10.1086/148307.

[2] Ivan Agullo, Dimitrios Kranas, and V Sreenath. "Large scale anomalies in the CMB and non-Gaussianity in bouncing cosmologies". In: *Classical and Quantum Gravity* 38.6 (Feb. 2021), p. 065010. DOI: 10.1088/1361-6382/abc521. URL: https://dx.doi.org/10.1088/1361-6382/abc521.

[3] Xingang Chen. "Primordial Non-Gaussianities from Inflation Models". In: *Adv. Astron.* 2010 (2010), p. 638979. DOI: 10.1155/2010/638979. arXiv: 1002.1416 [astro-ph.CO].

[4] Robert G. Crittenden and Neil Turok. "Looking for a Cosmological Constant with the Rees-Sciama Effect". In: *Phys. Rev. Lett.* 76 (4 Jan. 1996), pp. 575–578. DOI: 10.1103/PhysRevLett.76.575. URL: https://link.aps.org/doi/10.1103/PhysRevLett.76.575.

[5] G. Hinshaw et al. "FIVE-YEAR WILKINSON MICROWAVE ANISOTROPY PROBE* OBSERVATIONS: DATA PROCESSING, SKY MAPS, AND BASIC RESULTS". In: *The Astrophysical Journal Supplement Series* 180.2 (Feb. 2009), p. 225. DOI: 10.1088/0067-0049/180/2/225. URL: https://dx.doi.org/10.1088/0067-0049/180/2/225.

[6] Planck Collaboration et al. "Planck 2018 results - VI. Cosmological parameters (Corrigendum)". In: *Astronomy & Astrophysics* 652 (2021), p. C4. DOI: 10.1051/0004-6361/201833910e. URL: https://doi.org/10.1051/0004-6361/201833910e.

[7] P. J. E. Peebles and J. T. Yu. "Primeval adiabatic perturbation in an expanding universe". In: *Astrophys. J.* 162 (1970), pp. 815–836. DOI: 10.1086/150713.

[8] D. J. Fixsen. "THE TEMPERATURE OF THE COSMIC MICROWAVE BACKGROUND". In: *The Astrophysical Journal* 707.2 (Nov. 2009), p. 916. DOI: 10.1088/0004-637X/707/2/916. URL: https://dx.doi.org/10.1088/0004-637X/707/2/916.

[9] Wayne Hu and Naoshi Sugiyama. "Anisotropies in the Cosmic Microwave Background: an Analytic Approach". In: *The Astrophysical Journal* 444 (May 1995), p. 489. DOI: 10.1086/175624. arXiv: astro-ph/9407093 [astro-ph].

[10] D. J. Fixsen et al. "Calibration of the COBE FIRAS Instrument". In: *The Astrophysical Journal* 420 (Jan. 1994), p. 457. DOI: 10.1086/173577.

[11] Marc Kamionkowski, Arthur Kosowsky, and Albert Stebbins. "A Probe of Primordial Gravity Waves and Vorticity". In: *Phys. Rev. Lett.* 78 (11 Mar. 1997), pp. 2058–2061. DOI: 10.1103/PhysRevLett.78.2058. URL: https://link.aps.org/doi/10.1103/PhysRevLett.78.2058.

[12] Silvia Galli et al. “CMB polarization can constrain cosmology better than CMB temperature”. In: *Phys. Rev. D* 90 (6 Sept. 2014), p. 063504. DOI: 10.1103/PhysRevD.90.063504. URL: https://link.aps.org/doi/10.1103/PhysRevD.90.063504.

[13] P. A. R. Ade et al. “Improved Constraints on Primordial Gravitational Waves using Planck, WMAP, and BICEP/Keck Observations through the 2018 Observing Season”. In: *Phys. Rev. Lett.* 127 (15 Oct. 2021), p. 151301. DOI: 10.1103/PhysRevLett.127.151301. URL: https://link.aps.org/doi/10.1103/PhysRevLett.127.151301.

[14] The Planck Collaboration. *The Scientific Programme of Planck*. 2006. arXiv: astro-ph/0604069 [astro-ph].

[15] R. K. Sachs and A. M. Wolfe. “Perturbations of a cosmological model and angular variations of the microwave background”. In: *Astrophys. J.* 147 (1967), pp. 73–90. DOI: 10.1007/s10714-007-0448-9.

[16] E. Moura-Santos et al. “A Bayesian Estimate of the CMB–large-scale Structure Cross-correlation”. In: *The Astrophysical Journal* 826.2 (July 2016), p. 121. DOI: 10.3847/0004-637X/826/2/121. URL: https://dx.doi.org/10.3847/0004-637X/826/2/121.

[17] Albert Einstein. “Cosmological Considerations in the General Theory of Relativity”. In: *Sitzungsber. Preuss. Akad. Wiss. Berlin (Math. Phys.)* 1917 (1917), pp. 142–152.

[18] Y. Choquet-Bruhat. *General Relativity and the Einstein Equations*. Oxford Mathematical Monographs. OUP Oxford, 2008. ISBN: 9780191578854. URL: https://books.google.com.br/books?id=UjHbm5rfpi8C.

[19] Suman Sarkar, Biswajit Pandey, and Rishi Khatri. “Testing isotropy in the Universe using photometric and spectroscopic data from the SDSS”. In: *Monthly Notices of the Royal Astronomical Society* 483.2 (Nov. 2018), pp. 2453–2464. ISSN: 0035-8711. DOI: 10.1093/mnras/sty3272. eprint: https://academic.oup.com/mnras/article-pdf/483/2/2453/27184728/sty3272.pdf. URL: https://doi.org/10.1093/mnras/sty3272.

[20] Biswajit Pandey and Suman Sarkar. “Testing homogeneity of the galaxy distribution in the SDSS using Renyi entropy”. In: *Journal of Cosmology and Astroparticle Physics* 2021.07 (July 2021), p. 019. DOI: 10.1088/1475-7516/2021/07/019. URL: https://dx.doi.org/10.1088/1475-7516/2021/07/019.

[21] Edwin Hubble. “A Relation between Distance and Radial Velocity among Extra-Galactic Nebulae”. In: *Proceedings of the National Academy of Science* 15.3 (Mar. 1929), pp. 168–173. DOI: 10.1073/pnas.15.3.168.

[22] Georges Lemaitre. “A Homogeneous Universe of Constant Mass and Growing Radius Accounting for the Radial Velocity of Extragalactic Nebulae”. In: *Annales Soc. Sci. Bruxelles A* 47 (1927), pp. 49–59. DOI: 10.1007/s10714-013-1548-3.

[23] S. Dodelson and F. Schmidt. *Modern Cosmology*. Elsevier Science, 2020. ISBN: 9780128159484. URL: https://books.google.com.br/books?id=GGjfywEACAAJ.

[24] Verónica Motta et al. “Taxonomy of Dark Energy Models”. In: *Universe* 7.6 (2021), p. 163. DOI: 10.3390/universe7060163. arXiv: 2104.04642 [astro-ph.CO].

[25] Eric V. Linder. "Exploring the Expansion History of the Universe". In: *Phys. Rev. Lett.* 90 (9 Mar. 2003), p. 091301. DOI: 10.1103/PhysRevLett.90.091301. URL: https://link.aps.org/doi/10.1103/PhysRevLett.90.091301.

[26] Chao-Jun Feng et al. "A new class of parametrization for dark energy without divergence". In: *Journal of Cosmology and Astroparticle Physics* 2012.09 (Sept. 2012), p. 023. DOI: 10.1088/1475-7516/2012/09/023. URL: https://dx.doi.org/10.1088/1475-7516/2012/09/023.

[27] A. Hernández-Almada et al. "Stability analysis and constraints on interacting viscous cosmology". In: *Phys. Rev. D* 101 (6 Mar. 2020), p. 063516. DOI: 10.1103/PhysRevD.101.063516. URL: https://link.aps.org/doi/10.1103/PhysRevD.101.063516.

[28] A. Amariti et al. "Brane cosmology and the self-tuning of the cosmological constant". In: *Journal of Cosmology and Astroparticle Physics* 2019.10 (Oct. 2019), p. 007. DOI: 10.1088/1475-7516/2019/10/007. URL: https://dx.doi.org/10.1088/1475-7516/2019/10/007.

[29] Marc Kamionkowski and Adam G. Riess. "The Hubble Tension and Early Dark Energy". In: *Annual Review of Nuclear and Particle Science* 73.1 (2023), pp. 153–180. DOI: 10.1146/annurev-nucl-111422-024107. eprint: https://doi.org/10.1146/annurev-nucl-111422-024107. URL: https://doi.org/10.1146/annurev-nucl-111422-024107.

[30] Planck Collaboration et al. "Planck 2018 results - V. CMB power spectra and likelihoods". In: *Astronomy & Astrophysics* 641 (2020), A5. DOI: 10.1051/0004-6361/201936386. URL: https://doi.org/10.1051/0004-6361/201936386.

[31] M. Betoule et al. "Improved cosmological constraints from a joint analysis of the SDSS-II and SNLS supernova samples". In: *Astronomy & Astrophysics* 568, A22 (Aug. 2014), A22. DOI: 10.1051/0004-6361/201423413. arXiv: 1401.4064 [astro-ph.CO].

[32] Julian E. Bautista et al. "Measurement of baryon acoustic oscillation correlations at z = 2.3 with SDSS DR12 Lyα-Forests". In: *Astronomy & Astrophysics* 603, A12 (June 2017), A12. DOI: 10.1051/0004-6361/201730533. arXiv: 1702.00176 [astro-ph.CO].

[33] Alan H. Guth. "Inflationary universe: A possible solution to the horizon and flatness problems". In: *Phys. Rev. D* 23 (2 Jan. 1981), pp. 347–356. DOI: 10.1103/PhysRevD.23.347. URL: https://link.aps.org/doi/10.1103/PhysRevD.23.347.

[34] A.D. Linde. "A new inflationary universe scenario: A possible solution of the horizon, flatness, homogeneity, isotropy and primordial monopole problems". In: *Physics Letters B* 108.6 (1982), pp. 389–393. ISSN: 0370-2693. DOI: https://doi.org/10.1016/0370-2693(82)91219-9. URL: https://www.sciencedirect.com/science/article/pii/0370269382912199.

[35] Antony Lewis, Anthony Challinor, and Anthony Lasenby. "Efficient computation of CMB anisotropies in closed FRW models". In: *ApJ* 538 (2000), pp. 473–476. DOI: 10.1086/309179. arXiv: astro-ph/9911177 [astro-ph].

[36] Antony Lewis and Sarah Bridle. "Cosmological parameters from CMB and other data: A Monte Carlo approach". In: *PRD* 66 (2002), p. 103511. DOI: 10.1103/PhysRevD.66.103511. arXiv: astro-ph/0205436 [astro-ph].

[37] D. J. Fixsen et al. "Calibration of the COBE FIRAS Instrument". In: *The Astrophysical Journal* 420 (Jan. 1994), p. 457. DOI: 10.1086/173577.

[38] Planck Collaboration et al. "Planck 2013 results. XXVII. Doppler boosting of the CMB: Eppur si muove". In: *Astronomy & Astrophysics* 571 (2014), A27. DOI: 10.1051/0004-6361/201321556. URL: https://doi.org/10.1051/0004-6361/201321556.

[39] Esteban Ricardo Chalbaud Mogollón. *Kinematic effects and the break of statistical isotropy of the cosmic microwave background fluctuations*. 2021. DOI: https://doi.org/10.11606/D.43.2021.tde-31052021-162009.

[40] K. M. Górski et al. "HEALPix: A Framework for High-Resolution Discretization and Fast Analysis of Data Distributed on the Sphere". In: *ApJ* 622 (Apr. 2005), pp. 759–771. DOI: 10.1086/427976. eprint: astro-ph/0409513.

[41] José Carlos N. de Araujo. "The dark energy–dominated Universe". In: *Astroparticle Physics* 23.2 (2005), pp. 279–286. ISSN: 0927-6505. DOI: https://doi.org/10.1016/j.astropartphys.2004.12.004. URL: https://www.sciencedirect.com/science/article/pii/S0927650504002087.

[42] Robert G. Crittenden and Neil Turok. "Looking for a Cosmological Constant with the Rees-Sciama Effect". In: *Phys. Rev. Lett.* 76 (4 Jan. 1996), pp. 575–578. DOI: 10.1103/PhysRevLett.76.575. URL: https://link.aps.org/doi/10.1103/PhysRevLett.76.575.

[43] Niayesh Afshordi, Yeong-Shang Loh, and Michael A. Strauss. "Cross-correlation of the cosmic microwave background with the 2MASS galaxy survey: Signatures of dark energy, hot gas, and point sources". In: *Phys. Rev. D* 69 (8 Apr. 2004), p. 083524. DOI: 10.1103/PhysRevD.69.083524. URL: https://link.aps.org/doi/10.1103/PhysRevD.69.083524.

[44] S. P. Boughn and R. G. Crittenden. "The cross-correlation between the microwave and X-ray backgrounds: foregrounds and systematics". In: *Monthly Notices of the Royal Astronomical Society* 360.3 (July 2005), pp. 1013–1021. ISSN: 0035-8711. DOI: 10.1111/j.1365-2966.2005.09090.x. eprint: https://academic.oup.com/mnras/article-pdf/360/3/1013/3178164/360-3-1013.pdf. URL: https://doi.org/10.1111/j.1365-2966.2005.09090.x.

[45] S.P. Boughn and R.G. Crittenden. "A detection of the integrated Sachs–Wolfe effect". In: *New Astronomy Reviews* 49.2 (2005). Sources and Detection of Dark Matter and Dark Energy in the Universe, pp. 75–78. ISSN: 1387-6473. DOI: https://doi.org/10.1016/j.newar.2005.01.005. URL: https://www.sciencedirect.com/science/article/pii/S1387647305000096.

[46] Planck Collaboration et al. "Planck 2015 results - XXI. The integrated Sachs-Wolfe effect". In: *A&A* 594 (2016), A21. DOI: 10.1051/0004-6361/201525831. URL: https://doi.org/10.1051/0004-6361/201525831.

[47] A J Mead et al. “hmcode-2020: improved modelling of non-linear cosmological power spectra with baryonic feedback”. In: *Monthly Notices of the Royal Astronomical Society* 502.1 (Jan. 2021), pp. 1401–1422. ISSN: 0035-8711. DOI: 10.1093/mnras/stab082. eprint: https://academic.oup.com/mnras/article-pdf/502/1/1401/42438464/stab082.pdf. URL: https://doi.org/10.1093/mnras/stab082.

[48] Niayesh Afshordi, Yeong-Shang Loh, and Michael A. Strauss. “Cross-correlation of the cosmic microwave background with the 2MASS galaxy survey: Signatures of dark energy, hot gas, and point sources”. In: *Phys. Rev. D* 69 (8 Apr. 2004), p. 083524. DOI: 10.1103/PhysRevD.69.083524. URL: https://link.aps.org/doi/10.1103/PhysRevD.69.083524.

[49] O. Tange. “GNU Parallel 2018”. In: (Mar. 2018). URL: https://doi.org/10.5281/zenodo.1146014.

[50] Jesús Torrado and Antony Lewis. *Cobaya: Bayesian analysis in cosmology*. Astrophysics Source Code Library, record ascl:1910.019. Oct. 2019. ascl: 1910.019.

[51] Jesús Torrado and Antony Lewis. “Cobaya: code for Bayesian analysis of hierarchical physical models”. In: *Journal of Cosmology and Astroparticle Physics* 2021.05 (May 2021), p. 057. DOI: 10.1088/1475-7516/2021/05/057. URL: https://doi.org/10.1088%5C%2F1475-7516%5C%2F2021%5C%2F05%5C%2F057.

[52] George Casella and Edward I. George. “Explaining the Gibbs Sampler”. In: *The American Statistician* 46.3 (1992), pp. 167–174. ISSN: 00031305. URL: http://www.jstor.org/stable/2685208 (visited on 08/07/2023).